Unexpected Nonlinear Dynamics in NbN Superconducting Microwave Resonators

B. Abdo,* E. Segev, O. Shtempluck, and E. Buks
Microelectronics Research Center, Department of Electrical Engineering, Technion, Haifa 32000, Israel
(Dated: April 25, 2005)

In this work we characterize the unusual nonlinear dynamics of the resonance response, exhibited by our NbN superconducting microwave resonators, using different operating conditions. The nonlinear dynamics, occurring at relatively low input powers (2-4 orders of magnitude lower than Nb), and which include among others, bifurcations in the resonance curve, hysteresis loops and resonance frequency shift, are measured herein using varying temperature, applied magnetic field, white noise and rapid frequency sweeps. Based on these measurement results, we consider a hypothesis according to which Josephson junctions forming weak links at the boundaries of the NbN grains are responsible for the observed behavior, and we show that most of the experimental results are qualitatively consistent with such hypothesis.

PACS numbers: 85.25.-j, 74.50.+r, 47.20.Ky, 05.45.Xt

I. INTRODUCTION

Understanding the underlying mechanisms that cause and manifest nonlinear effects in superconductors has a significant importance both theoretically and practically. On the one hand, knowing how to minimize and control nonlinear effects, being the major cause for the degradation of performance of RF devices employing superconductors [1], would have a great technological impact. It will enable the design and fabrication of high performance superconducting RF devices with extended linear behavior, and higher power densities than afforded nowadays [2, 3]; On the other hand, identifying the origins of the nonlinearities in superconductors, would lead to a better understanding of the superconducting phenomena and its behavior in the microwave regime.

In spite of the intensive study of nonlinearities in superconductors in the past decades, we still lack a coherent picture regarding these effects and their origins [4]. This is partly because the nonlinear mechanisms in superconductors are various and many times act concurrently on the superconducting sample, hence making the identification process of the dominant factor mainly indirect and based on eliminations [5].

Nonlinear mechanisms in superconductors, which are usually divided into intrinsic and extrinsic origins, include among others, Meissner effect [6], pair-breaking, global and local heating effects [7, 8], rf and dc vortex penetration and motion [9], defect points, damaged edges [10], substrate material [11], and weak links [12]. Whereas weak links is a collective term representing various material defects located inside the superconductor such as weak superconducting points switching to normal state under low current density, Josephson junctions forming inside the superconductor structure, grain-boundaries, voids, insulating oxides, insulating planes. These defects and impurities generally affect the conduction properties of the superconductor and as a result cause extrinsic nonlinear effects.

Nonlinear effects in superconductors in general and in NbN in particular have been reported and analyzed by several research groups. Duffing like nonlinearity for example was observed in different superconducting resonators employing different geometries and materials. It was observed in a HTS parallel plate resonator [7], in a Nb microstrip resonator [13], in a Nb and NbN stripline resonators [3], in a YBCO coplanar-waveguide resonator [14], in a YBCO thin film dielectric cavity [8], and also in a suspended HTS thin film resonator [15]. Other nonlinearities including notches, anomalies developing at the resonance lineshape and frequency hysteresis can be found in [16, 17].

In this paper we report the observation of unexpected nonlinear dynamics measured in NbN superconducting microwave resonators. Among the observed effects, asymmetric resonances, multiple bifurcations in the resonance lineshape, hysteretic behavior in the vicinity of the bifurcations, hysteresis loops changing direction, resonance frequency shift as the input power is increased and nonlinear coupling. Some of these nonlinear effects were introduced in a previous publication [18], thus this paper will concentrate on presenting a different set of measurements applied to these nonlinear resonators, which provides a better understanding of the underlying physical mechanism causing these effects. For this purpose, we have measured the nonlinear superconducting resonators under different operating conditions, such as added white noise (to the main signal), fast frequency sweep using frequency modulation (FM), applied magnetic field, and varying temperature. Under each one of these operating conditions we observe interesting nonlinear dynamics, which qualitatively agree with our hypothesis of microscopic Josephson junctions forming at the boundaries of the NbN columnar structure.

The remainder of this paper is organized as follows, the fabrication process of the NbN superconducting resonators is described briefly in Sec. II. A short summary of previous results is brought in Sec. III. The nonlin-

*Electronic address: baleegh@tx.technion.ac.il

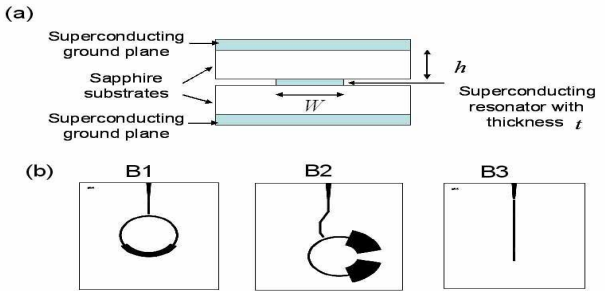

FIG. 1: (a) Schematic cross section of the stripline resonator used, consisting of five layers: two superconducting ground planes, two sapphire substrates and a NbN film in the middle deposited on one of the sapphires. (b) Top view of the three resonator layouts (B1, B2, B3) which were deposited as the middle layer.

ear dynamics of these microwave resonators measured under various operating conditions are reviewed in Sec. IV. Whereas possible underlying physical mechanisms responsible for the measured effects are discussed in Sec. V, which also concludes this paper.

II. FABRICATION PROCESS

The measurement results presented in this paper belong to three nonlinear NbN superconducting microwave resonators. The resonators were fabricated using stripline geometry, consisting of two superconducting ground planes, two sapphire substrates, and a deposited strip in the middle (the deposition was done on one of the sapphire substrates). Fig. 1 shows a schematic diagram illustrating stripline geometry and a top view of the three resonators layouts. For convenience we will be referring to the three resonators in the text by the shortened names B1, B2 and B3 as defined in Fig. 1. The sapphire substrates dimensions used were 34mm X 30mm X 1mm, whereas the coupling gap between the resonators and their feedline was set to 0.4mm in B1 and B3 cases and 0.5mm in B2 resonator. The resonators were dc-magnetron sputtered in a mixed Ar/N_2 atmosphere, near room temperature. The patterning was done using standard UV photolithography process, whereas the NbN etching was performed by Ar ion-milling. The sputtering parameters, design consideration as well as other fabrication details can be found elsewhere [18]. The critical temperature T_c of B1, B2 and B3 resonators were relatively low and equal to 10.7K, 6.8K and 8.9K respectively. The thickness of the NbN resonators were 2200 Å in B1, 3000 Å in B2, and 2000 Å in B3 resonator.

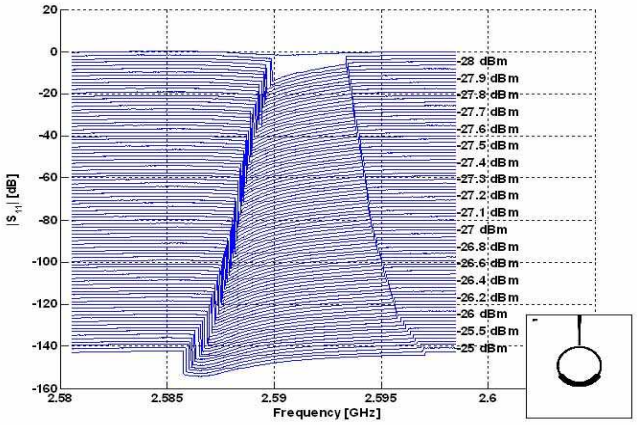

FIG. 2: S_{11} amplitude measurement of B1 resonator at its first mode $\sim$ 2.59GHz. The measured resonance lineshapes are asymmetrical and contain two abrupt bifurcations at the sides of the resonance. Moreover the bifurcation frequencies shift outwards as the input power is increased. The measured resonance lineshapes were shifted vertically by a constant offset for clarity. The layout of B1 resonator is depicted in the inset.

III. SUMMARY OF PREVIOUS RESULTS

As we have shown comprehensively in a previous publication [18], two of the main nonlinear features observed in our NbN nonlinear superconducting resonators are bifurcations that appear in the resonance curves at relatively low input powers and hysteresis loops forming in the vicinity of the bifurcations. In Fig. 2 we present a S_{11} parameter measurement of B1 first mode resonance featuring bifurcations at both sides of the resonance curve.

Furthermore, the frequencies at which the bifurcations occur shift outwards from the center frequency as the input power is increased. The measurement was performed, at liquid helium temperature 4.2K, using vector network analyzer. The measured curves in the figure were shifted vertically by a constant offset for clarity. In contrast to the nonlinear dynamics presented in Fig. 2, we show in Fig. 3, a resonance response measured at 4.2K, exhibiting Duffing nonlinearity of the kind generally reported in the literature [3, 14, 15]. This nonlinearity which can be explained in terms of resistance change ΔR and kinetic inductance change ΔL_K [19, 20] was measured at the first resonance frequency of a 2200 Å thickness Nb resonator employing B2 layout geometry (T_c = 8.9K). The differences between the two nonlinear dynamics are obvious, but nevertheless note the difference in the order of magnitude of the input powers at which these two nonlinearities occur, ~ -28 dBm in the NbN case vs. $\sim$ 10 dBm in the Nb resonator. In Fig. 4 we present a S_{11} measurement of B2 resonator at its second mode, measured while sweeping the frequency in both direc-

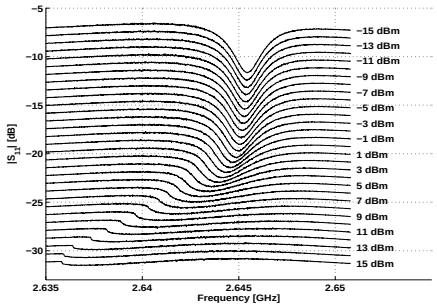

FIG. 3: Duffing nonlinearity exhibited by a Nb stripline resonator employing B2 layout at its first mode. The different S_{11} amplitude plots correspond to different input powers, ranging from −15 dBm to 15 dBm in steps of 2 dBm. As the input power is increased the resonance becomes asymmetrical and infinite slope develops at the left side of the resonance curve. The plots were offset in the vertical direction for clarity.

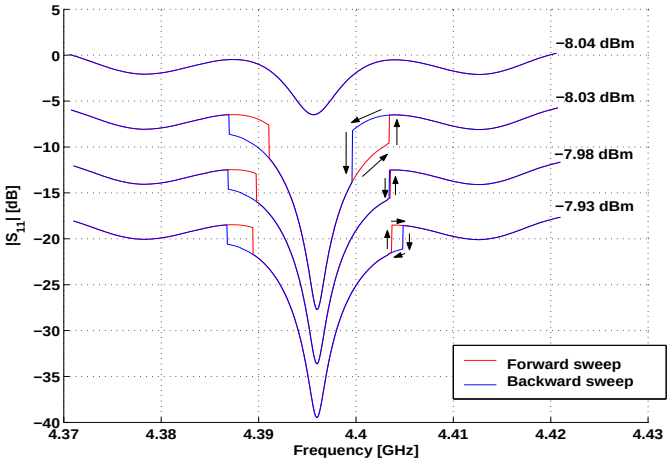

FIG. 4: Frequency sweep measurement of B2 resonator at $\sim$ 4.395GHz performed in both frequency directions. The plots exhibit hysteresis loops forming at the vicinity of the bifurcations, as well as hysteresis loops changing direction as the input power is increased. The red line represents a forward sweep, whereas the blue line represents a backward sweep. The resonance lineshapes were shifted vertically by a constant offset for clarity.

tions. The red line represents a forward frequency sweep whereas the blue line represents a backward frequency sweep. The graphs corresponding for different input powers were also offset in the vertical direction for clarity. At −8.04 dBm the resonance is linear and shows no hysteresis behavior. As the input power is increased by a power step of 0.01 dBm, to −8.03 dBm the resonance response lineshape is changed dramatically, featuring two bifurcations at both sides of the resonance curve and hysteresis loops forming in the vicinity of the bifurcations (as can be clearly seen in the figure). Moreover this measurement exhibits another interesting nonlinear feature. The right side hysteresis loop changes direction as the input power is increased. Between −8.03 dBm and −7.98 dBm the hysteresis loop circulates counter clockwise. At −7.98 dBm the hysteresis loop vanishes. Whereas as the input power is increased further, the loop circulates clockwise. Furthermore at −6.35 dBm (not shown here) the hysteresis loop vanishes again and changes its direction one more time, (it starts circulating counter clockwise as the power is increased).

In Fig. 5 we show yet another nonlinear feature exhibited by these nonlinear resonators, namely multiple bifurcations in the resonance curve. The figure plots the resonance response of B3 resonator at its first resonance frequency, corresponding to 1.49 dBm input power. The measurement which was obtained by sweeping the frequency axis in the forward and backward directions, features three bifurcations and hysteresis loops within the resonance lineshape in each direction.

Other experimental data featuring these effects and similar nonlinearities observed in B1, B2 and B3 resonators can be found in Ref. [18]. Among the nonlinearities not brought here or in [18], one can name, nonlinear coupling [21], and intermodulation gain [22].

IV. MEASUREMENT RESULTS

In the following subsections we present measurement results of B1 and B2 resonators, under different operating conditions. In subsection A, the impact of white noise power on the bifurcation feature is briefly examined. The dependence of the nonlinear dynamics on temperature varying and applied magnetic field are investigated in subsections B and C respectively. In subsection D, heating effects are considered through frequency sweep time analysis and comparisons to heating time scales previously reported in the literature. Evidence of the columnar structure of our NbN films is presented in subsection E. Possible interpretations of these observations are discussed in Sec. V.

A. WHITE NOISE EFFECT

Bifurcations in the resonance response of nonlinear oscillators is usually described in terms of metastable states and dynamic transition between basins of attraction of the oscillator [23]. Thus in order to examine qualitatively the metastability of the resonance bifurcations of these nonlinear resonators, we have applied a constant white noise power to the resonator, several orders of magnitude lower than the main signal power, using the setup shown in Fig. 6. The white noise level applied was −58 dBm/Hz. It was generated by amplifying the thermal noise of a room temperature 50 Ω load using an amplifying stage. The generated noise was added to the

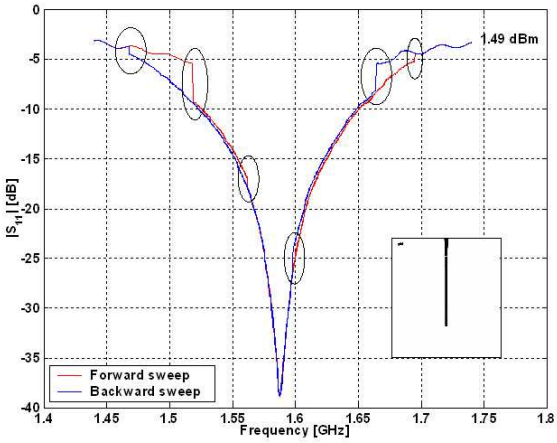

FIG. 5: S_{11} parameter amplitude measurement of the first resonance of B3 resonator, (shown in the inset), measured at input power of 1.49 dBm. The measurement was done using a network analyzer employing 4000 measurement points in each direction. The red line represents a forward frequency scan whereas the blue line represents a backward scan. The plot shows clearly three bifurcations within the resonance lineshape in each direction, as indicated by small circles.

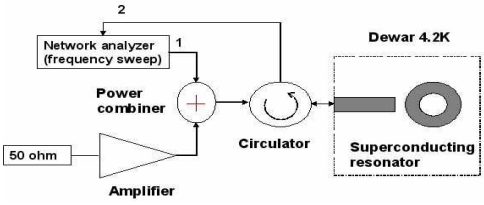

FIG. 6: Schematic diagram of the experimental setup used to measure the nonlinear resonance 2.585 GHz of B1 using frequency sweep mode while applying −58 dBm white noise.

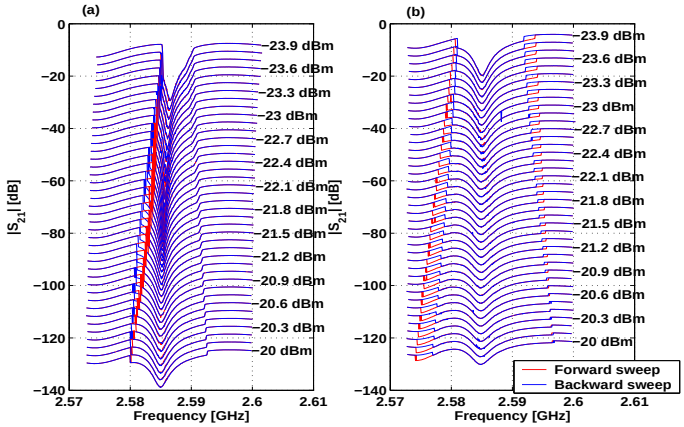

FIG. 7: Frequency sweep measurement of B1 resonator at 2.585 GHz performed in both directions (a) while applying white noise of −58 dBm/Hz (b) without applying external noise (∼ −80 dBm/Hz). The red line represents a forward sweep, whereas the blue line represents a backward sweep. The measured resonance curves were shifted vertically by a constant offset for clarity.

transmitted power of the network analyzer via a power combiner. The power reflections were redirected by a circulator on their way back, and were measured at the second port of the network analyzer, thus measuring S_{21} parameter. The effect of the −58 dBm/Hz white noise power on B1 first mode bifurcations, is shown in Fig. 7 (a), whereas for comparison in Fig. 7 (b) we show nearly noiseless (∼ −80 dBm/Hz) resonance curve measurements performed using the simple setup depicted in Fig. 6 without the amplifier and the combiner stage. The two measurements were carried out within the same input power range (−23.9 dBm through −20 dBm).

By comparing between the two measurement results, one can observe the following, the two fold bifurcations in Fig. 7 (b) form a hysteresis loop at each side of the resonance curve. In Fig. 7 (a) in contrast, as a result of the added noise, the bifurcations at the left side, represented by the thick colored lines on the graphs, become frequent and bidirectional, whereas the hysteresis loops, at the right side, vanish.

The transition rate $\Gamma(f)$ between the oscillator basins of attraction (as a function the oscillator frequency f), can be generally estimated by the expression [23] $\Gamma(f) = \Gamma_0 \exp\left(-E_A(f)/k_B T_{eff}\right)$, where $E_A(f)$ is the quasi-activation energy of the oscillator, T_{eff} is proportional to the noise power, k_B is Boltzmann's constant, f is the oscillator frequency, whereas Γ_0 is related to Kramers low-dissipation form [24] and it is given approximately by f_0/Q, where f_0 is the natural resonance frequency, and Q is the quality factor of the oscillator. Based on the results presented in Fig. 7, one can evaluate the following parameters $f_0 \simeq 2.585$GHz, $Q \sim 1620$, $\Gamma_0 \sim 1.6$MHz, $T_{eff} \sim 10^{14}$K. Whereas E_A the quasi-activation energy of the oscillator may be roughly estimated for the left and right sides of the resonance response separately. For the right side of the resonance curve, the quenching of the hysteresis as a result of the white noise, suggests that the applied noise power −58 dBm/Hz is within the high noise limit, where the noise power is higher than the energy barrier associated with this bifurcation. Whereas for the left side, the hysteresis loop and the noise-induced transitions, indicate that the noise power −58 dBm/Hz is still in the moderate noise limit, where the noise power is less than the quasi-activation energy associated with this bifurcation.

B. TEMPERATURE DEPENDENCE

The physical properties of superconductors such as London penetration depth, surface resistance and kinetic inductance are strongly dependent on temperature [25].

Whereas temperature varying measurements are generally used in the characterization process of superconductors and in the determination of London penetration depth [26], we vary the temperature here in order to examine its effect on the nonlinear dynamics of the resonators. The measurements were performed at temperature ranges well below T_c of the resonators, thus the exhibited nonlinear dynamics presented here are features of the superconducting phase only. In Fig. 8 subplot (a) we show a S_{11} parameter amplitude measurement versus frequency of B1 resonator attained at its third resonance mode [18]. The input power was set to -16.9 dBm, a power level at which the bifurcation is already present in the resonance curve, afterwards the temperature was increased from 5.4K through 8K in steps of 0.1K. The nonlinear dynamics of the resonance curve as the temperature is increased exhibit three main nonlinear features, the resonance frequency shifts towards lower frequencies, the bifurcation step decreases and the bifurcation frequency becomes lower. Whereas the first nonlinear feature can be explained in terms of increase in the resonator inductance per unit length L due to temperature rise [25], the second and third features are less straightforward, and are more likely related to the effect of temperature on the underlying nonlinear mechanism responsible for the observed effects. Likewise in subplot (b), B2 resonator at its second mode exhibits a similar behavior, though the input power applied in this case is -10 dBm, which is lower than the bifurcation threshold of this resonance (~ -9 dBm). Similarly the resonance frequency shifts gradually towards lower frequencies as the ambient temperature is varied from 5.4K through 5.9K in steps of 0.01K. Moreover at 5.8K, the resonator even achieves critical coupling condition ($S_{11} \simeq 0$) via temperature varying only.

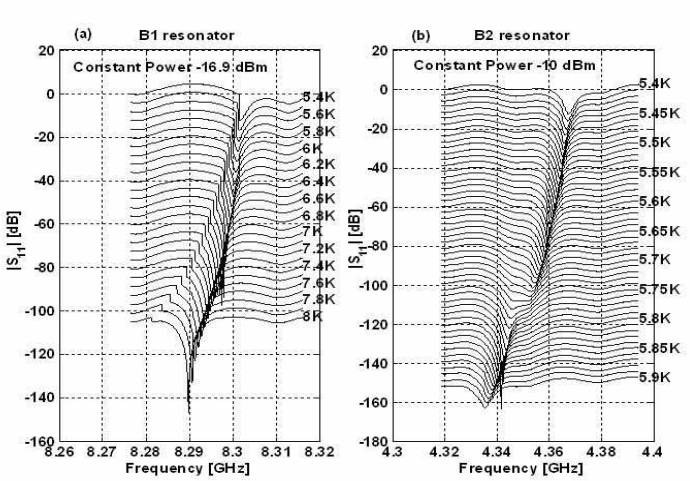

FIG. 8: Subplot (a) exhibits the nonlinear resonance frequency response of B1 measured under constant input power of -16.9 dBm while increasing the temperature from 5.4K through 8K in steps of 0.1K. In addition to the gradual resonance frequency shift, one can notice the resonance evolution as the temperature increases. Subplot (b) shows B2 second mode measured at a constant input power of -10 dBm while increasing the temperature from 5.4K through 5.9K in steps of 0.01K. In addition to the gradual resonance frequency shift, one can notice a temperature induced critical coupling occurring at 5.8K. The resonance curves were shifted vertically by a constant offset for clarity.

C. MAGNETIC FIELD DEPENDENCE

In order to better examine the extrinsic origin of the observed nonlinearities, we have investigated the dependence of the nonlinear resonances on magnetic field. The magnetic field dependence was measured by applying two methods, one by setting a constant input power and varying the magnetic field, and two by setting a constant magnetic field and varying the input power. The magnetic field applied was perpendicular to the resonator plane. The magnetic field measurements exhibiting B2 second resonance mode are summarized in Figs. 9, 10. In order to obtain the results of Fig. 9 we have applied a constant input power of -5 dBm to the resonator, and measured its S_{11} response while increasing the applied magnetic field by small steps. Above some low magnetic field threshold of 11.8mT, the left side bifurcation vanishes, thus suggesting that the physical mechanism causing the bifurcations is sensitive to low magnetic field. In Fig. 10 we applied the second method, where we set the magnetic field to a constant level of 0.09T and measured the resonance response while increasing the input power. The dynamic behavior measured using this method, as the input power is increased, undergoes through the following sequential phases, symmetrical and Lorentzian curves, resonance curves containing an upward bifurcation, a curve without bifurcation, and finally resonance curves containing a downward bifurcation.

D. FREQUENCY SWEEP TIME ANALYSIS

Resistive losses and heating effects are typically characterized by relatively long time scales [7, 17]. In attempt to consider whether such effects are responsible for the observed nonlinearities in general and for the bifurcations in particular, we have run frequency sweep time analysis using the experimental setup depicted in Fig. 11. We have controlled the frequency sweep cycle of an Anritsu model signal generator via FM modulation. The FM modulation was obtained by feeding the Anritsu with a saw tooth waveform generated by another signal generator having $1/f$ sweep time cycle. The reflected power from the resonator was redirected using a circulator and measured by a power diode and oscilloscope. The left and right hand bifurcations of B2 ~ 4.39GHz resonance were measured using this setup, while applying increasing FM modulation frequencies: $1, 10, 20, 30, 40, 50, 100, 150$

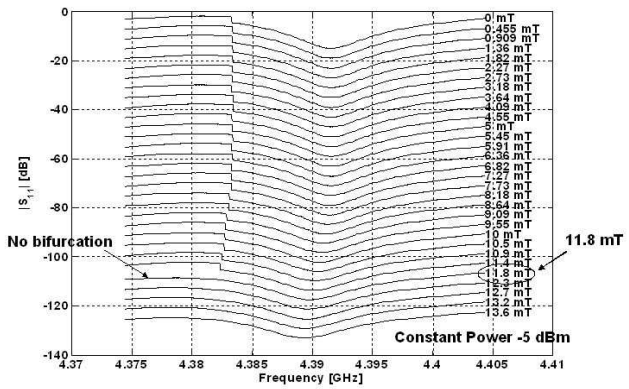

FIG. 9: Increasing the magnetic field gradually from zero causes the bifurcation in the B2 resonance band to disappear at relatively low value of 11.8mT, while applying a constant input power level of −5 dBm. This bifurcation vanishing indicates that the bifurcation mechanism is sensitive to magnetic field. The measured curves were shifted vertically by a constant offset for clarity.

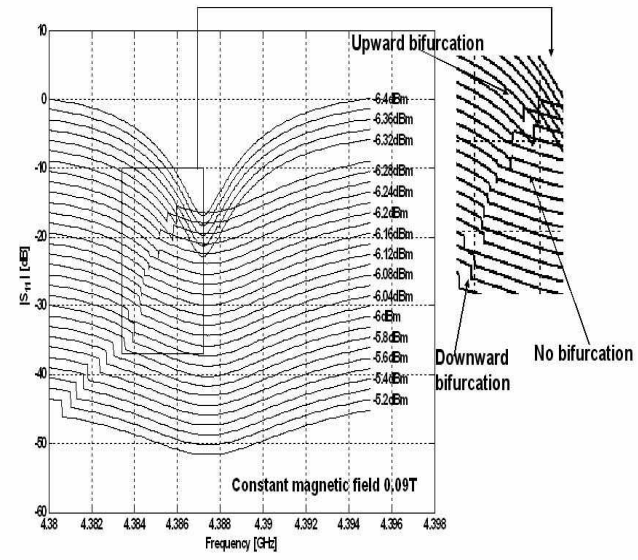

FIG. 10: B2 nonlinear resonance response measured under a constant magnetic field of 0.09T, while increasing the input power. The figure exhibits additional dependencies of the resonance response curves on applied magnetic field. The resonance which starts as a Lorentzian develops into a resonance curve having an upward bifurcation as the power is increased, afterwards into a curve with no bifurcation, followed by a resonance curve having a downward bifurcation as the input power is increased further. The measured curves were shifted vertically by a constant offset for clarity.

and 200kHz. In Fig. 12 we present a measurement result obtained at 50kHz FM modulation, or alternatively T_{sweep} of 20μs. The FM modulation applied was ±20MHz around 4.4022GHz center frequency. The measured resonance response appears inverted in the figure due to the negative output polarity of the power diode. The fact that both bifurcations continue to occur within the resonance lineshape (see Fig. 12), in spite of the short duty cycles that are on the order of $\sim \mu$s, indicates that heating processes which have typical time scale on the order of s to ms [7] are unlikely to cause these effects. Though there are also few who reported a smaller time constant of about 3μs [8] as a result of local heating effects.

In order to obtain an estimated low limit of local heating time scales in our NbN films, we apply a simple hot spot heating model to the resonators [27, 28, 29]. By further assuming that the substrate is isothermal and that the hot spot is dissipated mainly down into the substrate rather than along the film [27], one can evaluate the characteristic relaxation time of the hot spot using the equation $\tau = Cd/\alpha$, where C is the heat capacity of the superconducting film (per unit volume), d is the film thickness, and α is the thermal surface conductance between the film and the substrate [28]. Substituting for our B2 NbN resonator yields a characteristic relaxation time of $\tau \simeq 5.4 \cdot 10^{-8}$s, where the parameters $C \simeq 2.7 \cdot 10^{-3}\mathrm{Wcm}^{-3}\mathrm{K}^{-1}$ (NbN) [29], $d = 3000$Å (B2 thickness), and $\alpha \simeq 1.5\mathrm{Wcm}^{-2}\mathrm{K}^{-1}$ at 4.2K (sapphire substrate) [29], have been used. Similar calculation based on values given in Ref. [27] yields $\tau \simeq 2.1 \cdot 0^{-9}$s. These time scales are of course 2-3 orders of magnitude lower than the time scales examined by the FM modulation setup.

Nevertheless intermodulation products observed in these resonators [22], which generally require fast nonlinear response for their generation on the order of $\leq 10^{-10}$s [3], further excludes heating effects, though not entirely those associated with very fast heating mechanisms similar to hot spots for example.

E. COLUMNAR STRUCTURE

It is well known from numerous research works done in the past [30, 31], that NbN films can grow in a granular columnar structure under certain deposition conditions. Such columnar structure may even promote the growth of random built-in Josephson junctions at the grain boundaries of the NbN films. To study the NbN granular structure we have sputtered about 2200Å thickness NbN film on a thin small rectangular sapphire substrate of 0.2 mm thickness. The sputtering conditions applied were similar to those used in the fabrication of B2 resonator. Following the sputtering process, the thin sapphire was cleaved, and a scanning electron microscope (SEM) micrograph was taken at the cleavage plane. The SEM micrograph in Fig. 13 which clearly shows the columnar structure of

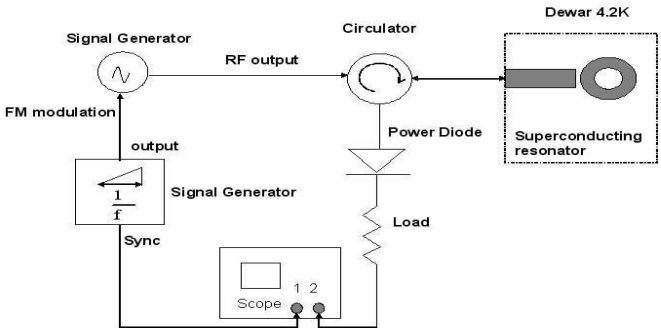

FIG. 11: Frequency sweep time analysis setup. The frequency sweep time of the microwave signal generator was FM modulated by a saw tooth waveform with frequency f. The reflected power from the resonator was measured by a power diode and oscilloscope.

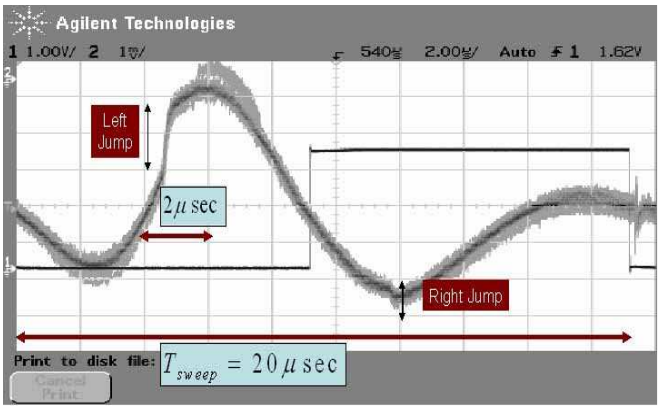

FIG. 12: Frequency sweep time measurement. The figure displays the resonance measured by Agilent oscilloscope while applying a saw tooth FM modulation of frequency 50kHz (T_{sweep} =20μs) to the signal generator. The left and right bifurcations of the resonance are still apparent in spite of the fast rate frequency sweep. Thus indicating that the bifurcations do not originate from any global heating mechanism.

the deposited NbN film and its grain boundaries, further supports our weak link hypothesis. The typical diameter of each NbN column is about 20 nm.

V. DISCUSSION

As we argue herein the physical mechanism that may potentially account for the nonlinear dynamics of these NbN resonators, is the extrinsic weak link mechanism, or more specifically Josephson junctions forming at the columnar structure boundaries of the NbN films. In addition, we show that this hypothesis is qualitatively consistent with some of our measurement results.

The measurement results which support the Josephson junction hypothesis can be summarized as follows:

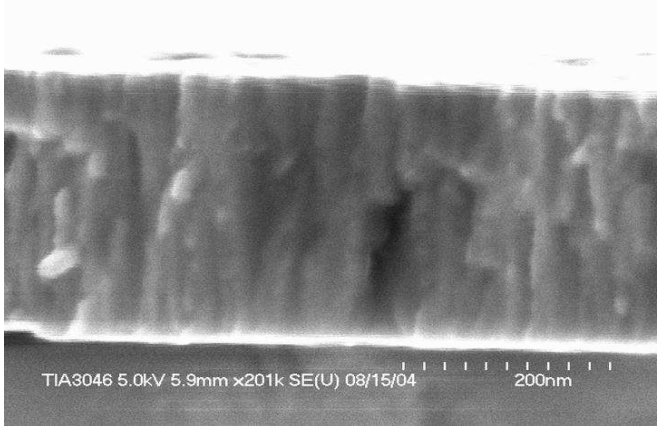

FIG. 13: SEM micrograph displaying a 2200Å NbN film deposited on a thin sapphire substrate using similar sputtering conditions as B2 resonator. The micrograph exhibits clearly the columnar structure of the NbN film and its grain boundaries.

(a) The columnar structure of the NbN films and their grain boundaries demonstrated in Fig. 13, which may allow the formation of Josephson junctions between the NbN grains.

(b) The onset of bifurcations and nonlinear features occurring at considerably low input power levels, about 2-4 orders of magnitude lower than the onset of Duffing nonlinearity in the Nb resonator (~ -28 in Fig. 2 versus $\sim$ 10 dBm in Fig. 3). This low power threshold highly implies an extrinsic nonlinear origin. Such extrinsic nonlinearity could be ac driven Josephson junctions, having low onset of instability amplitude, or junctions characterized by a low Josephson critical current, resulting in bifurcations in the dynamics of the gauge invariant phase difference across the Josephson junctions, at relatively low ac current amplitudes [32].

(c) The bifurcation dependence on magnetic field as was shown in Fig. 9, where B2 resonance bifurcation vanished as the perpendicular magnetic field was increased above some low magnetic field threshold $\sim$ 11.8 mT, which is about 3.5 times lower than H_{c_1} of NbN reported for example in [3]. On the other hand Josephson junctions are known for their sensitive dependence on magnetic field.

(d) The observation of a very small number of bifurcations in the resonance lineshape, (two in Figs. 2, 4 and three in Fig. 5), compared to the large number of built in Josephson junctions expected according to the columnar structure model, may be explained qualitatively by one of the following possible scenarios. The coupling between the Josephson junctions and the global resonator activates only a small number of Josephson junctions characterized by some limiting properties such as Josephson resonance frequency falling within the resonance band of the global resonator, or Josephson onset of instability amplitude being lower than the driving oscillation

amplitude inside the resonator. Whereas the other scenario assumes a synchronization mechanism acting on the junctions, thus causing them to lock and evolve with the same frequency. Such synchronization mechanism may be similar to the mechanism recently analyzed in Ref. [33], where synchronization between nonlinear oscillators is achieved through nonlinear frequency pulling and reactive coupling.

(e) The rapid frequency sweep experiments, which excluded most heating effects (except possible very fast local heating mechanisms), further supports the Josephson junction hypothesis, since dynamic states of ac biased Josephson junctions may involve very little dissipation (vanishing dc voltage).

Moreover it was shown in several experimental works published recently [34, 35, 36, 37], examining the resonance lineshape of a radio frequency resonators coupled to a superconducting ring containing a single Josephson junction, that interesting nonlinear dynamics can develop in the RF circuit resonance response as the external magnetic flux applied through the ring is varied. Among the nonlinear dynamics reported therein one can name, bifurcations in the resonance lineshape, single and opposed fold bifurcations (hysteresis loops) [34], pinch resonances, where the opposed fold resonances appear to touch (pinch off) [35], and even stochastic jumps [36]. These experimental results are shown to be solutions of the nonlinear equations of motion for the system. In addition, different solutions of the nonlinear equation of Josephson junction driven by ac field, for various limiting cases, can be found in Ref. [32]. Whereas the nonlinear dynamics of Josephson junctions incorporated in resonant cavities, which was analyzed recently in several theoretical and experimental studies, mainly for the purpose of developing sources of coherent microwave radiation, can be found in Refs. [38, 39, 40, 41, 42], and in the cited references therein. Although these works do not analyze the effect of Josephson junctions on the resonance response of the cavity (a single mode is generally assumed), they provide a good understanding of the I-V characteristics of these arrays.

In spite of the qualitative arguments presented here, a large part of the underlying physics of these nonlinear resonators is still not fully understood, and further theoretical work may be needed in order to account for most of the experimental data reported here.

ACKNOWLEDGEMENTS

B.A. would like to thank John R. Clem for bringing to his attention some recent work done on Josephson junctions. E.B. would especially like to thank Michael L. Roukes for supporting the early stage of this research and for many helpful conversations and invaluable suggestions. Very helpful conversations with Oded Gottlieb, Gad Koren, Emil Polturak, and Bernard Yurke are also gratefully acknowledged. This work was supported by the German Israel Foundation under grant 1-2038.1114.07, the Israel Science Foundation under grant 1380021, the Deborah Foundation and Poznanski Foundation.

[1] Z. Ma, E. de Obaldia, G. Hampel, P. Polakos, P. Mankiewich, B. Batlogg, W. Prusseit, H. Kinder, A. Anderson, D. E. Oates, R. Ono, and J. Beall, IEEE trans. Appl. Supercond. **7**, 1911 (1997).
[2] R. B. Hammond, E. R. Soares, B. A. Willemsen, T. Dahm, D. J. Scalapino, and J. R. Schrieffer, J. Appl. Phys. **84**, 5662 (1998).
[3] C. C. Chen, D. E. Oates, G. Dresselhaus and M. S. Dresselhaus, Phys. Rev. B. **45**, 4788 (1992).
[4] D.E. Oates, M. A. Hein, P. J. Hirst, R. G. Humphreys, G. Koren, and E. Polturak, Physica C. **372-376**, 462 (2002).
[5] M. A. Golosovsky, H. J. Snortland, and M. R. Beasley, Phys. Rev. B. **51**, 6462 (1995).
[6] S. K. Yip and J. A. Sauls, Phys. Rev. letts. **69**, 2264 (1992).
[7] L. F. Cohen, A. L. Cowie, A. Purnell, N. A. Lindop, S. Thiess, and J. C. Gallop, Supercond. Sci. and Technol. **15**, 559 (2002).
[8] J. Wosik, L.-M. Xie, J. H. Miller, Jr., S. A. Long, and K. Nesteruk, IEEE Trans. Appl. Supercond. **7**, 1470 (1997).
[9] D. E. Oates, H. Xin, G. Dresselhaus, and M. S. Dresselhaus, IEEE Trans. Appl. Supercond. 11, 2804 (2001).
[10] B. B. Jin and R. X. Wu, J. of Supercond. **11**, 291 (1998).
[11] A. V. Velichko, D. W. Huish, M. J. Lancaster, and A. Porch, IEEE Trans. Appl. Supercond. **13**, 3598 (2003).
[12] J. Halbritter, J. Appl. Phys. **68**, 6315 (1990).
[13] A. L. Karuzskii, A. E. Krapivka, A. N. Lykov, A. V. Perestoronin, and A. I. Golovashkin, Physica B **329-333**, 1514 (2003).
[14] Z. Ma, E. D. Obaldia, G. Hampel, P. Polakos, P. Mankiewich, B. Batlogg, W. Prusseit, H. Kinder, A. Anderson, D. E. Oates, R. Ono, and J. Beall, IEEE Trans. Appl. Supercond. **7**, 1911 (1997).
[15] B. A. Willemsen, J. S. Derov, J. H. Silva, S. Sridhar, IEEE Trans. Appl. Supercond. **5**, 1753 (1995).
[16] A. M. Portis, H. Chaloupka, M. Jeck, and A. Pischke, Superconduct. Sci. & Technol . **4**, 436 (1991).
[17] S. J. Hedges, M. J. Adams, and B. F. Nicholson, Elect. Lett. **26**, 977 (1990).
[18] B. Abdo, E. Segev, Oleg Shtempluck, and E. Buks, cond-mat/0501114.
[19] T. Dahm and D. J. Scalapino, J. Appl. Phys. **81**, 2002 (1997).
[20] J. H. Oates, R. T. Shin, D. E. Oates, M. J. Tsuk, and P. P. Nguyen, IEEE Trans. Appl. Supercond. **3**, 17 (1993).
[21] B. Abdo, E. Segev, O. Shtempluck, and E. Buks, cond-mat/0501236.
[22] B. Abdo, E. Segev, O. Shtempluck, and E. Buks, unpublished.

[23] J. S. Aldridge and A. N. Cleland, cond-mat/0406528.
[24] H. A. Kramers, Physica **7**, 284 (1940).
[25] D. M. Sheen, S. M. Ali, D. E. Oates, R. S. Withers, and J. A. Kong, IEEE Trans. Appl. Supercond. **1**, 108 (1991).
[26] B. W. Langley, S. M. Anlage, R. F. W. Pease, and M. R. Beasley, Rev. Sci. Instrum. **62**, 1801 (1991).
[27] M. W. Johnson, A. M. Herr, and A. M. Kadin, J. Appl. Phys. **79**, 7069 (1996).
[28] A. M. Kadin and M. W. Johnson, Appl. Phys. Lett. **69**, 3938 (1996).
[29] K. Weiser, U. Strom, S. A. Wolf, and D. U. Gubser, J. Appl. Phys. **52**, 4888 (1981).
[30] S. Isagawa, J. Appl. Phys. **52**, 921 (1980).
[31] Y. M. Shy, L. E. Toth, and R. Somasundaram, J. Appl. Phys. **44**, 5539 (1973).
[32] J. McDonald and J. R. Clem, Phys. Rev. B. **56,** 14723 (1997).
[33] M. C. Cross, A. Zumdieck, R. Lifshitz, and J. L. Rogers, Phys. Rev. Lett. **93**, 224101 (2004).
[34] R. Whiteman, J. Diggins, V. Schollmann, T. D. Clark, R. J. Prance, H. Prance, and J. F. Ralph, Phys. Letts. A **234**, 205 (1997).
[35] H. Prance, T. D. Clark, R. Whiteman, R. J. Prance, M. Everitt, P. Stiffel, and J. F. Ralph, cond-mat/0411139.
[36] R. J. Prance, R. Whiteman, T. D. Clark, H. Prance, V. Schollmann, J. F. Ralph, S. Al-Khawaja, and M. Everitt, Phys. Rev. Letts. **82**, 5401 (1999).
[37] T. D. Clark, R. J. Prance, R. Whiteman, H. Prance, M. J. Everitt, A. R. Bulsara, and J. F. Ralph, cond-mat/0411139.
[38] E. Almaas and D. Stroud, Phys. Rev. B. **65**, 134502 (2002).
[39] E. Almaas and D. Stroud, Phys. Rev. B. **67**, 064511 (2003).
[40] I. Tornes and D. Stroud, cond-mat/0501147.
[41] J. G. Caputo and L. Loukitch, cond-mat/0501660.
[42] P. Barbara, A. B. Cawthrone, S. V. Shitov, and C. J. Lobb, Phys. Rev. Letts. **82**, 1963 (1999).